CO_3^{-2} complexes is significantly greater for HREE (Peppard *et al.*, 1962). Kosterin (1959), suggests that decreasing pressure, fixation of CO_3^{-2}, or a change in alkalinity, are possible reasons for REE complexes to break down and facilitate precipitation. Mineyev (1963), in a study of the Kazakhstan massif, showed that a decrease in Na^+ content of hydrothermal fluids due to albitization would cause precipitation of REE-fluoride. This process might also have been partly responsible for the HREE enrichment in the albitites and albite pegmatites, due to the presence of small amounts of fluorite.

4.2.5. Conclusions

The similarity in REE data from the various intrusions analysed confirms the geochemical and petrographic studies, which suggested that the albitized intrusions are genetically related to the intrusive granodiorites of the Murchison schist belt. The albitized intrusions represent the hydrothermally altered cupolas of granodiorite intrusions which originally had a composition similar to that of the Willie pluton.

The process of albitization within the intrusion does not induce major changes in the REE distribution of the host rock unless intense mass replacement and carbonatization occur due to a high fluid to rock ratio, such as in the Malati Store intrusion. The albitizing fluids were probably enriched in HREE, relative to the cooling granodiorite from which they were derived, due to the presence of suitable complexing ligands such as CO_3^{2-}, which would preferentially complex with the HREE. The precipitation of carbonate minerals induces the destabilization of the CO_3^{2-}-HREE complexes, resulting in HREE-enrichment of the cupola zones of the granodiorite intrusions. The presence of carbonate minerals and small amounts of fluorite in the albitized intrusions and the albite pegmatites, suggests that Fl^- as well CO_3^{-2} might have been important complexing agents. Limited experimental data also indicate that gold may also be transported as a carbonate complex (Boyle, 1979). Studies of vein Au-W deposits support the involvement of dilute CO_2 fluids and the possibility of carbonate complexation of gold and tungsten (Kerrich and Fyfe, 1981).

The albite pegmatites are the product of a post-magmatic fluid phase, derived from the cooling granodiorite, into which stable HREE complexes and other incompatible elements were preferentially concentrated. The REE data suggest that the albite pegmatites related to emerald mineralization are genetically related to the Willie pluton or its equivalent.

4.3. Sulphide Geochemistry

4.3.1 Introduction

Euhedral pyrite is the dominant sulphide mineral within the albitized granodiorite intrusions and the associated auriferous pyritic schists. The sulphide petrography is described in detail in Chapter 3. The geochemistry of the pyrites was examined in order to document their geochemical characteristics and to asses whether a relationship exists between pyrite in the granitoid rocks and in the associated auriferous schists. Meyer *et al.* (1985), conducted a study on pyrites from various primary Archaean gold deposits, as well as from allogenic pyrites from various early Proterozoic sedimentary basins in southern Africa, and this data has been used for comparison. Samples of pyrite were obtained from the Malati Store and Discovery Shaft intrusions and from the pyritic schist at Discovery Shaft Mine. Pyrite samples were also obtained from the albite pegmatites associated with emerald mineralization within the Cobra and Discovery pits at GEM. Two samples of pyrite were obtained from the ore and the spatially related albitized intrusion at the Minerva mine. Two samples of pyrite from the Antimony Line were also analysed. A sample of cubic pyrite was obtained from the ultramafic schists at GEM, which are apparently unrelated to mineralization, and this sample is assumed to represent either diagenetic or metamorphic pyrite.

The Co and Ni contents and, more importantly, the Co:Ni ratios in pyrite, have been found to be valuable indicators for discriminating between pyrites and for providing information about their genesis and province (Bralia *et al.*, 1979; Bajwah *et al.*, 1987). The geochemistry of pyrites has been studied by many workers, mainly in an attempt to elucidate the genesis of pyritic ores (Mitchel, 1968 and Bralia *et al.* 1979). Recent studies have shown:

1. that the cobalt content in pyrites associated with Cu-rich massive sulphide deposits is higher than in pyrite from equivalent Pb-Zn rich systems (Price, 1972),
2. that the Ni content of pyrite tends to increase with increasing basicity of the host rock (Botinelly *et al.*, 1985),
3. that during metamorphism, cobalt is concentrated in pyrite and Ni in pyrrhotite (Bralia *et al.*, 1979),
4. that the Co content of remobilized pyrite (during post depositional hydrothermal events) decreases, while Ni contents remain almost unchanged (Bralia *et al.*, 1979; Walsh and Solomon, 1981) and.

5. that diagenetic pyrite is distinguished from epigenetic, hypogene pyrite, by higher contents of Co and Ni (Scott, 1986).

4.3.2. Analytical Procedures

Samples containing disseminated pyrite were gently crushed to the average size of the pyrites and concentrated by heavy medium separation. The pyrites were liberated from the adherent silicate matrix by hydrofluoric acid treatment (Neuerberg, 1975) and then cleaned in hydrochloric acid and finally distilled water. The pyrites were then hand-picked under a binocular microscope. Care was taken not to include other minerals, especially gold and, in the case of the Malati Store samples, arsenopyrite and stibnite. The samples were then analysed by instrumental (epithermal) neutron activation analysis (NAA). Samples of 70-150 mg were used for analysis. A well homogenised duplicate sample (MUL.1) was prepared and analysed in separate irradiation runs in the reactor to check for any systematic inaccuracies with the system. The results were found to be in good agreement (Table 4.3.1), with the maximum difference being 15.5%.

Element	MUL.1A	MUL.1B	Average	% Error
Cr (ppm)	483.24	492	487.62	1.80
Ni (ppm)	78.59	67.13	72.86	8.40
Co (ppm)	118.48	125.98	122.23	8.50
Au (ppm)	19.55	16.93	18.24	15.50
Sb (ppm)	980	1080	1030	10.20
As (ppm)	395	445	420	12.60

Table 4.3.1. RESULTS OF A DUPLICATE ANALYSIS FOR SAMPLE MUL.1 SHOWING PERCENTAGE ERRORS

The sulphides were also mounted and examined microscopically for various inclusions and mineral intergrowth (See Chapter 3.0).

4.3.3 Co, Ni and Cr Contents

Table 4.3.2 shows the trace element content of the pyrites from the Discovery Shaft and Malati Store intrusions. Table 4.3.3 shows the pyrite trace element content from the Discovery Shaft pyritic schist, albite pegmatites, Minerva Mine intrusion, the Antimony Line and diagenetic pyrite from Discovery pit. The statistical treatment of the data is shown in Table 4.3.4. The cobalt contents for the pyrites examined range from 45 ppm to 463 ppm. The Minerva intrusion had the highest average Co contents (424.1 ppm and 450.0 ppm).

Discovery Shaft Intrusion (DSI)								
Sample	Cr (ppm)	Ni (ppm)	Co (ppm)	Co/Ni	Au (ppm)	Sb (ppm)	As (ppm)	(Co/Co+Ni) *1000
11.11	281.66	187.06	463.43	2.48	6.23	0.48	24.78	712.41
12.3	416.21	356.34	285.30	0.80	96.42	0.90	40.38	444.64
KE21.21	322.02	266.72	335.72	1.16	24.38	0.37	9.83	537.63
D.2	254.65	216.39	260.15	1.20	15.02	0.30	11.23	545.91
KE51.14	330.85	392.18	239.64	0.61	3.89	0.20	58.20	378.29
KE51.6	456.16	478.29	337.90	0.71	60.43	0.78	50.30	414.00
D.6	331.92	203.40	262.10	1.29	132.45	0.34	17.23	563.05
KE51.4	337.51	420.13	320.58	0.76	1.23	0.80	58.50	432.80
DIS.4	357.87	321.46	314.20	0.98	32.40	0.59	36.56	494.27
DIS.5	389.48	265.51	296.77	1.12	16.96	0.36	18.50	529.38
Average	345.83	312.96	311.78	1.11	38.94	0.51	32.75	506.34
Malati Store Intrusion (MSI)								
Sample	Cr (ppm)	Ni (ppm)	Co (ppm)	Co/Ni	Au (ppm)	Sb (ppm)	As (ppm)	(Co/Co+Ni) *1000
MD4.193	405.20	88.39	189.59	2.14	78.25	60.50	570	682.03
MD4.192	206.90	51.56	111.09	2.15	22.69	32.20	299	683.00
MUL.1	467.62	72.86	122.23	1.68	18.24	10.30	420	626.53
MUL.2	296.60	60.57	119.09	1.97	37.45	2000	433	622.66
MUL.3	358.76	49.58	139.66	2.82	30.99	23.11	170	737.99
MUL.4	324.93	76.35	107.46	1.41	83.96	4000	840	584.60
MUL.5	452.29	122.89	132.64	1.08	50.41	40.54	395	519.08
MD3.164	332.96	85.90	162.36	1.89	46.19	66.39	429	653.96
Average	368.04	76.01	136.51	1.89	46.28	906.83	419	643.76

Table 4.3.2. Cr, Ni, Co, Au, Sb AND As CONTENTS OF PYRITES FOR THE DISCOVERY SHAFT AND MALATI STORE INTRUSIONS

Discovery Shaft Pyritic Schist (DPS)								
Sample	Cr (ppm)	Ni (ppm)	Co (ppm)	Co/Ni	Au (ppm)	Sb (ppm)	As (ppm)	(Co/Co+Ni) *1000
7.2B	346.06	73.32	45.29	0.62	400.72	0.17	18.06	381.84
G.2	300.81	98.74	49.62	0.50	78.12	0.13	9.53	334.46
DIS.4	387.41	132.19	74.85	0.57	532.01	0.63	18.17	361.52
ORE.4	332.46	129.06	87.88	0.68	121.42	0.37	17.15	405.09
ORE.10	398.86	171.71	72.69	0.42	98.41	0.46	12.87	297.42
Average	353.12	121.00	66.07	0.56	246.14	0.35	15.16	356.07
Albite Pegmatites								
Samples	Cr (ppm)	Ni (ppm)	Co (ppm)	Co/Ni	Au (ppm)	Sb (ppm)	As (ppm)	(Co/Co+Ni) *1000
COB.1	364.81	80.94	131.80	2.16	24.59	0.45	12.80	683.49
COB.2	350.68	79.42	140.79	1.77	31.39	0.52	18.50	639.34
COB.3	286.21	140.79	232.21	1.65	19.46	0.32	10.10	622.31
PIT.5	342.19	89.41	159.42	1.79	25.78	0.56	17.50	640.68
Average	336.97	92.68	166.81	1.84	24.56	0.46	14.73	646.46
Minerva Mine Intrusion (MMI)								
Sample	Cr (ppm)	Ni (ppm)	Co (ppm)	Co/Ni	Au (ppm)	Sb (ppm)	As (ppm)	(Co/Co+Ni) *1000
MVA.4	350.66	222.10	424.12	1.91	1.59	0.65	212	656.31
MVA.5	396.37	254.13	460.33	1.77	3.56	0.31	314	639.26
Antimony Line Pyrite (ALP)								
Sample	Cr (ppm)	Ni (ppm)	Co (ppm)	Co/Ni	Au (ppm)	Sb (ppm)	As (ppm)	Co/Co+Ni) *1000
ANT.3	320.45	80.24	145.41	1.81	26.87	49.21	216	644.41
ANT.5	354.46	79.45	154.90	1.94	32.15	59.45	321	660.97
Diagenetic Pyrite (Discovery Pit)								
PIT.23	900.31	1074	668.17	0.62	1.25	0.14	5.30	383.53

Table 4.3.3. Cr, Ni, Co, Au, Sb and As CONTENTS OF PYRITE FROM THE DISCOVERY SHAFT ORE ZONE, ALBITE PEGMATITES, MINERVA MINE INTRUSION, ANTIMONY LINE AND DIAGENETIC PYRITE FROM DISCOVERY PIT.

Nickel (ppm)	MSI	DSI	DPS	ABP	MMI	MPS
Sample Size	8	10	5	4	2	2
Average	76.04	312.96	121.00	92.68	238.11	148.70
Median	74.72	305.10	129.06	84.45	238.11	148.70
Mode	60.57	295.61	98.74	60.94	222.41	137.68
Geometric Mean	72.99	296.94	116.23	88.37	237.12	148.29
Std. Deviation	23.86	96.34	37.18	34.26	22.60	15.59
Minimum	49.56	187.06	73.32	60.94	222.10	137.68
Maximum	122.89	478.29	171.71	140.93	254.13	159.73
Chrome (ppm)	**MSI**	**DSI**	**DPS**	**ABP**	**MMI**	**MPS**
Sample Size	8	10	5	4	2	2
Average	358.04	345.84	353.12	335.97	374.52	272.37
Median	345.87	334.71	346.08	346.43	374.52	272.37
Mode	324.92	330.85	332.46	286.21	350.90	260.47
Geometric Mean	347.40	340.65	351.27	334.57	373.76	272.15
Std.Deviation	89.73	62.91	40.25	34.46	33.70	16.83
Minimum	206.90	254.65	300.81	286.21	350.88	260.47
Maximum	497.62	456.16	398.86	364.81	398.37	284.28
Cobalt (ppm)	**MSI**	**DSI**	**DPS**	**ABP**	**MMI**	**MPS**
Sample Size	8	10	5	4	2	2
Average	136.51	311.78	66.07	166.01	437.06	103.11
Median	127.43	306.49	42.69	150.10	437.06	103.11
Mode	119.09	295.30	60.12	131.62	424.12	97.01
Geometric Mean	133.20	306.75	64.01	161.65	436.86	92.14
Std.Deviation	26.03	62.84	18.02	45.14	18.30	8.62
Minimum	107.45	239.64	45.29	131.60	424.12	97.01
Maximum	169.56	463.43	87.88	231.21	450.10	109.10

MSI = Malati Store intrusion
DSI = Discovery Shaft intrusion
DPS = Discovery Shaft pyritic schist
ABP = Albite pegmatites
MMI = Minerva Mine intrusion
MPS = Minerva pyritic schist

Table 4.3.4. NICKEL, CHROME AND COBALT TRACE ELEMENT STATISTICS FOR PYRITE

The Discovery Shaft intrusion pyrites have a lower average cobalt content of 312 ± 63 ppm. The lowest average cobalt content was observed in the Discovery Shaft pyritic schist, with an average value of 66 ± 18 ppm. The albite pegmatite and the Malati Store intrusion have similarly low average Co values of 136 ppm and 166 ppm respectively. The Antimony Line pyrite has an average Co content 150 ppm, a value which fall in the range defined by the Malati Store pyrites.

The nickel content for the pyrites from the present study range from 50 ppm to 478 ppm. The Discovery Shaft intrusion has the highest average value of 313 ± 98 ppm. The Minerva intrusion pyrites shows high Ni contents of 222 ppm and 254 ppm. The Malati Store intrusion has the lowest average value of 76 ± 24 ppm. The pyrite from the albite pegmatites has a similar value of 93 ± 34 ppm. The Discovery Shaft pyritic schist has an average value of 121 ± 37 ppm, similar to the Minerva pyritic schist, with an average value of 103 ppm. The Antimony Line pyrites have an average Ni content of 79.8 ppm, and occur within the range defined by the Malati Store pyrites (76 ± 24 ppm). The diagenetic pyrite has a very high Ni concentration of 1074 ppm.

The average chrome values for all the deposits are similar, ranging between 351 ppm to 347 ppm. The diagenetic pyrite, however differs significantly, with a chrome content of 900 ppm. This pyrite sample has significantly higher Co, Ni and Cr contents, compared to the sulphides associated with epigenetic mineralization.

On the basis of a "Student's t test" there is no significant difference, at a 95% confidence level, between the Co, Ni and Cr contents of the Malati Store pyrites, those of the albite pegmatite pyrites and the Antimony Line pyrite. Similarly no significant difference exists between the Co and Ni contents of the Discovery pyritic schist and the Minerva pyritic schist. The cobalt and nickel contents however of the pyritic schist pyrites from Minerva and Discovery Shaft are significantly different compared to their spatially related intrusions.

4.3.4. Co:Ni ratios

The pyrites show a range of Co:Ni ratios from 0.42 to 2.58 (Table 4.3.2 and 4.3.3). Figure 4.3.1 shows a Co versus Ni plot for the pyrites, giving the fields of occurrence. The samples from the Discovery Shaft intrusion show the greatest range of Co:Ni ratios, from 0.61 to 2.48, with an average of 1.11. The samples define a fairly diffuse field around the Co:Ni = 1.0 line.

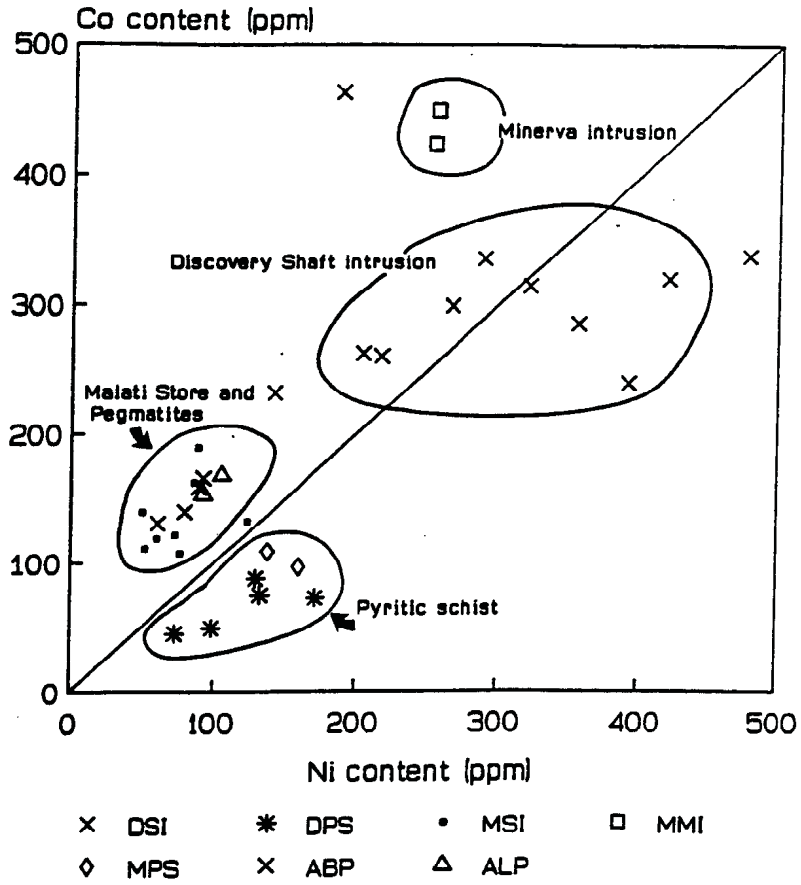

Figure 4.3.1. Plot of Co versus Ni content for the pyrites examined in this study
DSI - Discovery Shaft intrusion
DPS - Discovery Shaft pyritic schist
MSI - Malati Store intrusion
MMI - Minerva mine intrusion
MPS - Minerva mine pyritic schist
ABP - Albite pegmatites from GEM
ALP - Antimony Line pyrite

All the Malati Store pyrites have Co:Ni ratios >1.0 and range from 1.41 to 2.82, with a average of 1.89. The Minerva Mine intrusion pyrites have Co:Ni ratios of 1.91 and 1.77 and plot within the cobalt-rich field of the Discovery Shaft intrusion pyrites. The Discovery Shaft and Minerva pyritic schist pyrites have low Co:Ni ratios (< 1.0) ranging between 0.42 to 0.79, with an average of 0.56. These define a discrete field below the Co:Ni = 1.0 line. The albite pegmatite pyrites all have Co:Ni ratios >1.0 and an average ratio of 1.84. This value is similar to that of the Malati Store and Antimony Line pyrites and plots within the field defined by these samples. Figure 4.3.2 is a Co versus Ni plot showing the fields defined by the samples from this study, compared with both pyrites from hypogene sulphides from various Archaean mines, and from allogenic samples from the Central Rand Group (Meyer *et al.*, 1985).

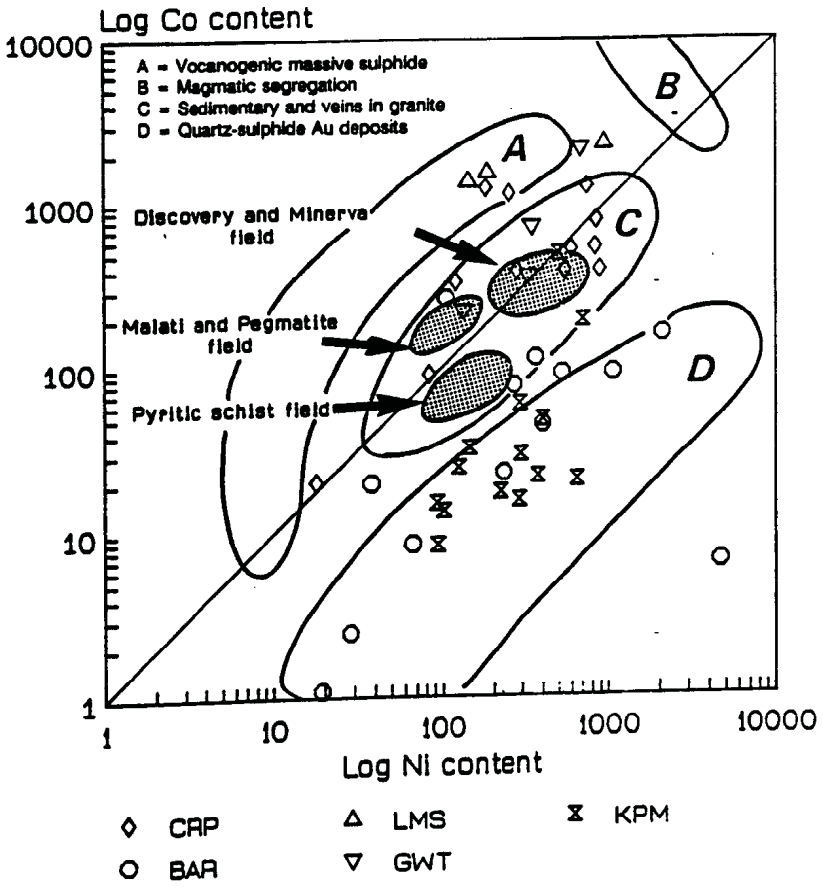

Figure 4.3.2. Plot of log Co versus log Ni content showing the "genetic fields" from Meyer *et al.* (1990) and the fields defined by the pyrites from this study. Various pyrite samples from Meyer *et al.* (1990) were used for comparison.
CRP - Central Rand Group allogenic pyrite
LMS - Letaba massive sulphide deposit
KPM - Klipwal gold mine
BAR - Barberton gold mines
GWT - Western Transvaal granitoids.

The fields delineating compositions typical for various deposits, as determined by Meyer *et al.* (1990.) are also plotted. All the samples from this study occur in the field defined by Meyer *et al.* (1990) as the "sedimentary and veins in granites" field (Figure. 4.3.2). The pyrite samples from the Klipwal and Barberton mines (Meyer *et al.*, 1985), scatter around a Co:Ni ratio of approximately 0.1, well below the area defined by the pyrites from this study, and within the field of "quartz-sulphide gold deposits". The former samples have similar Ni contents to the samples of this study, but have a reduced Co content and hence a lower Co:Ni ratio. Samples from the Letaba deposit in the Murchison Schist belt have a Co:Ni ratio of 3.08 and Co and Ni concentrations of 563 ppm and 183 ppm, respectively (Meyer *et al.*, 1985). These samples are from the volcanogenic massive sulphide deposits situated along the so called "Cu-Zn line", and plot within the volcanogenic field. The pyrites analysed from the Antimony Line have a Co:Ni ratio of 1.6 and 1.68 and plot within the field defined by the Malati Store and albite pegmatite

pyrites, suggesting that the mineralization is genetically related.

Figure 4.3.3. is a plot of Co versus Co:Ni ratios for the pyrites. The albite pegmatite pyrites, Malati Store pyrites and samples from the Antimony Line all plot within the same field. The Discovery Shaft intrusion and the pyritic schists also form discrete fields. The plot shows that the pyrites from the Murchison area differ significantly from the Barberton samples (Meyer *et al.*, 1990). The limited sampling from the Antimony Line shows that these pyrites are distinctly different from the samples of the Letaba Cu-Zn line. This has genetic significance for the mineralization of the Antimony Line, since the Co and Ni contents of the pyrites do not appear to have been derived by a volcanogenic exhalative process.

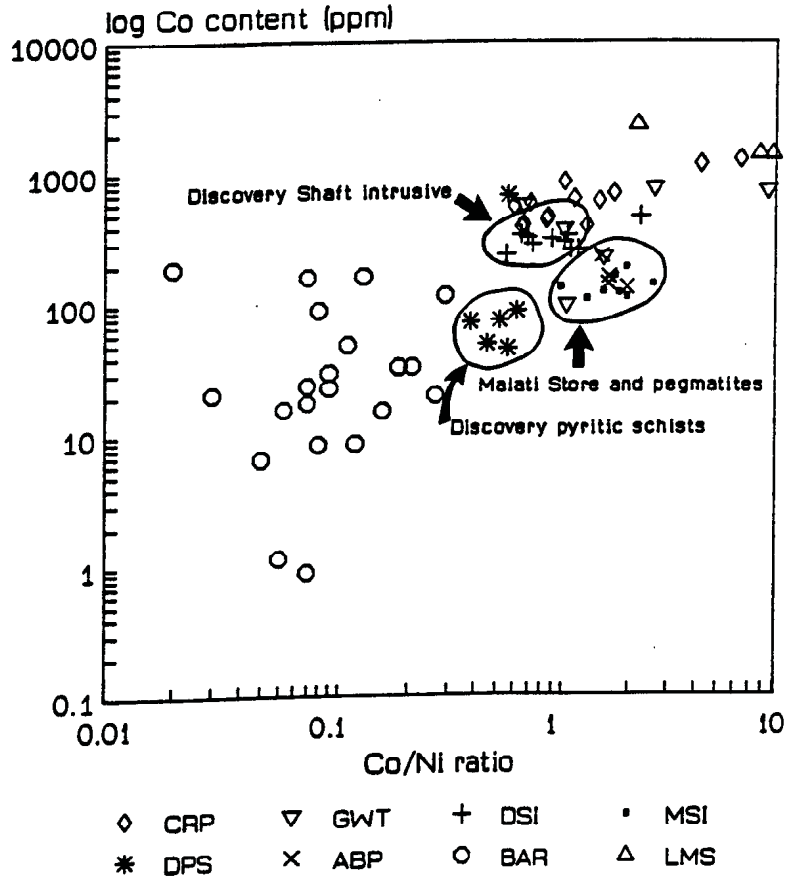

Figure 4.3.3. Plot of log Co versus Co:Ni ratio for the pyrites of this study compared to the data of Meyer *et al.* (1985). Symbols as per Figure 4.3.2.

4.3.5. Gold, Antimony and Arsenic Contents.

Tables 4.2.2 and 4.2.3 contain the Au, Sb and As values for the pyrites analysed. Table 4.3.5 shows the statistical treatment of this data. The gold content of the pyrites analysed is variable, ranging from 0.14 ppm to 532 ppm. The samples from the pyritic schist show the highest average Au values of 246 ± 185 ppm. The lowest gold value for the intrusions was obtained from the Minerva Mine intrusion, which has an average value of 2.6 ppm.

Antimony (ppm)	DSI	DSI	DPS	ABP	MMI	MPS
Sample Size	8	10	5	4	2	2
Average	908.2	0.51	0.35	0.46	0.48	0.63
Median	61.95	0.43	0.37	0.49	0.48	0.63
Mode	40.45	0.36	0.17	0.32	0.31	0.56
Geometric Mean	176.72	0.46	0.30	0.45	0.44	0.45
Std. Deviation	1439.3	0.24	0.21	0.11	0.24	0.39
Minimum	23.11	0.20	0.13	0.32	0.31	0.35
Maximum	4000	0.90	0.63	0.56	0.65	0.91

Gold (ppm)	MSI	DSI	DPS	ABP	MMI	MPS
Sample Size	8	10	5	4	2	2
Average	46.26	36.94	246.14	24.56	2.57	9.08
Median	42.82	20.66	121.42	23.78	2.57	9.08
Mode	30.99	16.96	96.41	21.59	1.59	2.59
Geometric Mean	40.79	18.47	181.87	21.19	2.37	6.30
Std. Deviation	24.26	44.14	185.32	5.21	1.30	9.16
Minimum	18.24	1.23	78.12	19.40	1.59	2.59
Maximum	83.96	132.45	532.01	31.39	3.56	15.58

Arsenic (ppm)	MSI	DSI	DPS	ABP	MMI	MPS
Sample Size	8	10	5	4	2	2
Average	433.25	32.81	15.16	14.73	226.86	207.50
Median	424.50	31.67	17.15	15.15	226.86	207.50
Mode	395	24.78	12.87	10.10	199.60	175.6
Geometric Mean	404.49	27.33	14.72	14.30	225.22	204.90
Std. Deviation	152.35	18.87	3.62	3.96	38.50	32.50
Minimum	170	9.83	9.53	10.10	212	175
Maximum	640	58.20	18.17	18.50	314	240

MSI = Malati Store Intrusion
DSI = Discovery Shaft Intrusion
DPS = Discovery pyritic schist
ABP = Albite pegmatite
MMI = Minerva Mine intrusion
MPS = Minerva pyritic schist

Table 4.3.5. ANTIMONY, GOLD AND ARSENIC TRACE ELEMENT STATISTICS FOR PYRITE

The diagenetic pyrite from GEM has the expected low value of 0.14 ppm. The Discovery shaft pyrites show the greatest range of gold content from 1.23 ppm to 132 ppm, with an average of 39 ppm.

The Discovery Shaft and Malati Store pyrites have similar average values of 38 ppm and 46 ppm respectively. The albite pegmatites have an average of 25 ± 5 ppm. It can be seen that the pyritic schist pyrites from the Discovery Shaft and Minerva deposits are enriched by a factor of 6 and 13 times, respectively, for gold, compared to the spatially related, albitized intrusions. The Antimony Line pyrite sample has a high gold content of 26.87 ppm, which is to be expected from pyrite in this gold mineralized environment.

Generally, the antimony content is low in all the pyrites except the Malati Store intrusion. The Malati Store pyrite samples show an extremely wide range of values, from 23.11 ppm to 4000 ppm. Although the data is limited there appears to be a bimodal distribution to the data, with extremely high values of >1000 ppm and other values of less than 100 ppm. The high antimony content samples are interpreted to represent those which contain visible stibnite or berthierite inclusions within the pyrite grain. The low content samples are interpreted to represent pyrite samples which do not contain visible antimony mineral phases and contain antimony minerals as microscopic inclusions, or possibly as antimony dissolved in the pyrite lattice. However, these lower values show enrichment in antimony (23-60 ppm) when compared to pyrites from the other deposits. The pyrite samples from the Antimony Line have a high value of 49 ppm and 59 ppm Sb, as would be expected from pyrite in this environment. The pyrites from the other deposits generally have low antimony content (<1 ppm).

Arsenic values are especially high in the Malati Store deposit, the average being 433 ± 152 ppm. This enrichment is thought to be due to the intimate relationship between arsenopyrite and pyrite in this deposit and reflects the high arsenic content of the pyrite, detected petrographically. The Antimony Line sample also has a high arsenic value of 216 ppm, which is in the range of the Malati Store pyrite. The pyritic schists and the albite pegmatite pyrites contain similar arsenic values, averaging 15.16 ppm and 14.74 ppm respectively, with a narrow range. The limited samples from the Minerva mine show high arsenic contents for both the pyritic schist (207 ppm) and the intrusive (263 ppm).

The antimony and arsenic contents of the Discovery Shaft intrusion, associated pyritic schist and albite pegmatite pyrites are similar at a 95 % confidence level and the gold content of the Malati Store and Discovery Shaft pyrites are also statistically similar.

4.3.6. Correlation Coefficients

Table 4.3.6. shows the correlation matrices for all the trace elements in the pyrites examined for each deposit. Good correlations generally exist between the gold and arsenic content in pyrites from all the deposits except the Discovery Shaft pyritic schist, where gold could not be correlated with any other element.

Gold could generally only be correlated with arsenic, although the albite pegmatite pyrites also showed an antimony-gold correlation. The Malati Store pyrites exhibit a positive correlation between arsenic and antimony, confirming the intimate nature observed petrographically between arsenopyrite and antimony minerals within the pyrite. The lack of correlation within the pyritic schists is due to late gold remobilization and fracture filling.

No significant correlation is present between the Co:Ni ratio and gold content of the pyrites, unlike that seen in the pyrite samples from the Barberton greenstone belt (Meyer *et al.*, 1985) (indicating a lack of sulphide redistribution). Positive cobalt-nickel correlations are only present in the Discovery Shaft pyrites and samples from the albite pegmatites. Figure 4.3.4 shows a plot of Co:Ni ratio versus the gold content of the pyrites for the pyrites examined. There is however a distinctly negative correlation for the combined data. ie. the pyrites with the lowest Co:Ni ratio have the highest gold content. This suggests that there has been a some redistribution of gold and an increase in the pyrites, especially within the pyritic schists. The lack of correlation within a deposit may be due to a lack of data quantity

Discovery Shaft Intrusion (DSI)

	Au	As	Sb	Ni	Co	Cr	Co/Ni
Au	1.00	**0.65**	0.23	-0.08	-0.29	0.41	-0.12
As	**0.65**	1.00	0.50	**0.84**	-0.10	0.44	-0.53
Sb	0.24	0.50	1.00	0.57	0.26	0.58	-0.25
Ni	-0.08	**0.84**	0.57	1.00	-0.18	**0.70**	**-0.76**
CO	-0.29	-0.10	0.26	-0.18	1.00	-0.18	**0.74**
Cr	0.41	0.44	0.58	**0.70**	-0.18	1.00	**-0.60**

Discovery Shaft Pyritic Schist (DPS)

	Au	As	Sb	Ni	Co	Cr	Co/Ni
Au	1.00	-0.15	0.41	-0.29	-0.11	0.40	0.33
As	-0.15	1.00	0.43	-0.14	0.32	0.38	**0.71**
Sb	0.41	0.43	1.00	**0.73**	**0.74**	**0.81**	-0.09
Ni	-0.29	-0.14	**0.73**	1.00	**0.73**	**0.67**	0.50
Co	-0.11	0.32	**0.74**	**0.73**	1.00	0.40	0.21
Cr	0.40	0.38	**0.81**	**0.67**	0.40	1.00	0.36

Malati Store Intrusion (MSI)

	Au	As	Sb	Ni	Co	Cr	Co/Ni
Au	1.00	**0.72**	0.43	0.45	0.37	0.07	-0.32
As	**0.72**	1.00	0.67	0.34	0.07	0.08	-0.54
Sb	0.43	0.67	1.00	-0.13	-0.55	-0.14	-0.37
Ni	0.45	0.34	-0.13	1.00	0.33	0.60	-0.76
Co	0.37	0.07	-0.55	0.33	1.00	0.13	0.27
Cr	0.07	0.08	-0.14	0.60	0.31	1.00	-0.36

Albite Pegmatites (ABP)

	Au	As	Sb	Ni	Co	Cr	Co/Ni
Au	1.00	**0.95**	**0.78**	-0.46	-0.58	0.51	-0.16
As	**0.95**	1.00	**0.94**	-0.54	-0.65	0.60	-0.06
Sb	**0.78**	**0.94**	1.00	**-0.70**	**-0.77**	**0.75**	0.19
Ni	-0.46	-0.45	**-0.70**	1.00	**0.99**	**-0.99**	**-0.80**
Co	-0.58	-0.65	**-0.77**	**0.99**	1.00	**-0.99**	**-0.71**
Cr	0.51	0.60	**0.75**	**-0.99**	**-0.99**	1.00	**0.76**

Table 4.3.6. CORRELATION MATRICES FOR PYRITE TRACE ELEMENTS

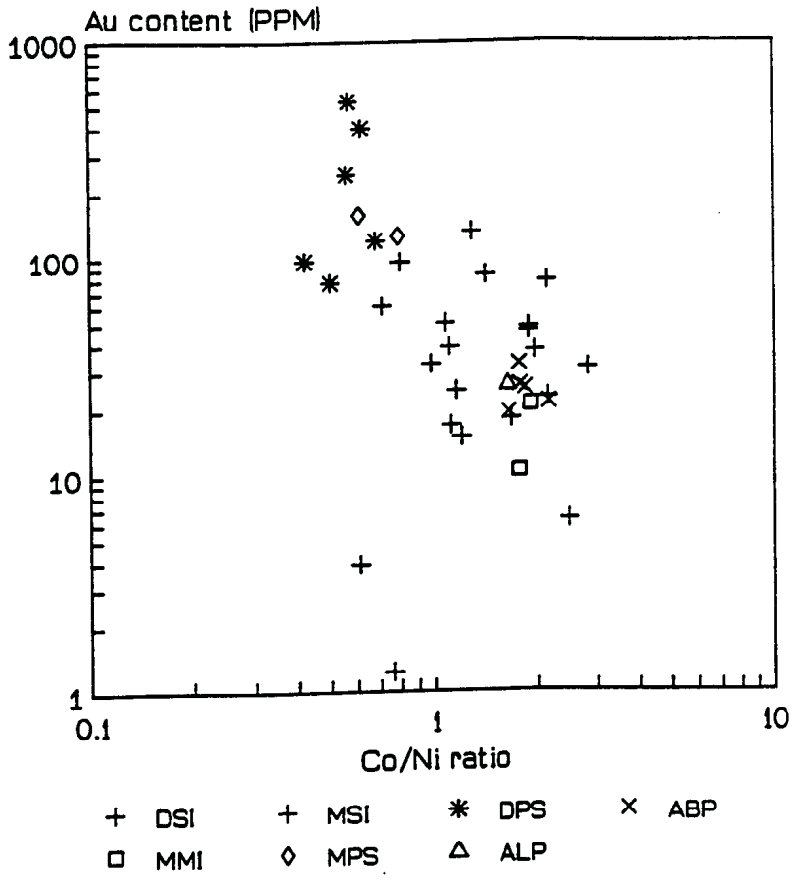

Figure 4.3.4. Plot of Au content versus the Co:Ni ratio for the pyrites from this study.
Symbols as per Figure 4.3.1.

4.3.7. Discussion

The cobalt and nickel disulphides, cattierite and vaesite, respectively, are isostructural and the similarity of their cell dimensions and bond lengths facilitates the development of complete solid solutions with pyrite. For most natural pyrites, Ni and Co occur in trace amounts and thus usually occur as isomorphous substitutions for Fe in the pyrite lattice. The distribution of Co and Ni in pyrite is governed by physiochemical conditions (Kullerud and Yoder, 1964), as well as by the availability of these metals during pyrite formation (Loftus-Hills and Solomon, 1967). The physiochemical processes which control the behaviour of trace elements in sulphides are very complex and are not well understood. Ghosh-Dastidar *et al.* (1970), in the investigation of trace elements in coexisting sulphides, found that the partition coefficients are also dependent on the element concentration and/or the presence of other trace elements in the phase considered, as well as the temperature. In general, the trace element content of hydrothermally deposited sulphides depends on several physiochemical parameters which

are known to vary in hydrothermal systems. Thus heterogeneous sulphides should be expected to occur within a single deposit. Lafitte and Maury (1983), suggest that post-formational processes, such as solid-state diffusion and recrystallization, may result in more homogeneous compositions. Recrystallization processes can result in increased purity of the minerals or a change in composition due to interactions with extraneous elements (Lafitte and Maury, 1983).

The dissolution of gold in sulphides is less precisely understood. Gold may occur within the pyrite as a solid solution, as layers within the pyrite growth planes, as microscopic crystals or along P-type charge defects within the pyrite lattice. Karauti (1941), investigated the nature of Au in pyrite and reported Au solubilities of up to 2000 ppm. Conflicting studies by McPheat *et al.* (1969) concluded that gold in auriferous pyrite exists in solid solution up to a concentration of 1 ppm and that the balance of the metal occurs as finely dispersed grains throughout the mineral. Iwanoff (1951) studied the distribution of gold in pyrite up to 1000 ppm Au and was able to demonstrate that the Au formed sub-microscopic inclusions with diameters of up to 0.01 microns. There are several different mechanisms which favour pyrite over other sulphides as a gold host, making surfaces or fractures in pyrite a preferred site deposition. Experimental data suggest that gold in solution in the pyrite lattice is limited and that the metal generally occurs as discrete, often sub-microscopic particles (McPheat *et al.*, 1986; Iwanoff, 1951). By virtue of the surface properties of pyrite, which are highly variable, gold can be incorporated by micro-plating into the crystal (Smith, 1942). Pyrite is a semi-conductor, well known for its variable conductive properties (Smith, 1942). In general, conductive properties reflect internal order in crystalline substances; in metals, increasing impurity produces changes in conduction type, with p-type conduction correlating strongly with lattice imperfection and disorder. Closer examination of the surface phenomena (Mironov *et al.*, 1981) showed that pyrite displays differing degrees of gold adsorption, which correlates with its semi-conductor properties. These properties in turn relate to purity and perfection of the crystal lattice (Smith, 1942). N-type conductivity can exist in well formed crystals, while impurities, commonly arsenic, accompany crystal defects and induce p-type conductivity within the lattice. The greatest adsorption of gold is shown by pyrites which have mixed p- and n-type conductivities. This is consistent with the knowledge that in synthesised semi-conductors, the greatest deposition of metals take place at p-n junctions. Experimental studies by Bancroft and Jean (1982), showed that gold has an affinity to pyrite and that metallic gold can be rapidly precipitated from solution onto the surface of pyrite grains from solutions of 10 ppm Au. Studies by Knipe

and Foster (1991) on Precambrian gold deposits have demonstrated the site-specific occurrence of gold and silver on the surface of pre-existing sulphide minerals. A two-stage mechanism for deposition has been proposed which includes adsorption (physical process) and the reduction of gold complexes onto the sulphide grain where ion exchange take place.

4.3.8. Conclusion

The use of the nickel-cobalt content and the Ni:Co ratio of pyrites to define the genetic association of the various deposits has proven to be a useful technique in the present study. The Co:Ni ratios were used to discriminate between the various mineralization deposits from this study and to confirm that the pyrites have granitic affinity and are distinctly different to the pyrites associated with Au mineralization, in for example, the Barberton greenstone belt.

The Malati Store intrusion and albite pegmatite pyrites have similar trace element geochemistry. This suggests that there is a genetic relationship between the fluids responsible for albitization and those that crystallized to form the pegmatites. The Malati intrusion is, however, enriched in As, Au and Sb compared to the pegmatites. The gold content of the Malati Store pyrites is statistically similar to that of the Discovery Shaft intrusion, suggesting that the gold-bearing fluids occurred early in sulphide precipitation and that more intense alteration (greater fluid/rock ratio) in the Malati Store intrusions did not introduce more gold or redistribute the gold.

Although the data is limited, there appear to be distinct similarities between the sulphides in the Malati Store intrusion, albite pegmatites and the sulphides of the Antimony Line. This suggests that there is a genetic relationship between the fluids responsible for the various mineralization. The pyrites of the Antimony Line thus have a granitic signature and are distinctly different to the pyrites in the volcanogenic massive sulphide-type deposits of the Cu-Zn line. This data militates against a volcanogenic origin for the Antimony Line and suggests a origin related to the mineralization within the granitoids.

Pyrites from the albitized intrusions and associated pyritic schists at Minerva Mine and Discovery Shaft show distinct chemical similarities which suggest similar genesis. The pyrites from the schists have greatly reduced cobalt contents and slightly reduced nickel contents compared to the associated mineralized intrusions. It is envisaged that the

pyritic schists developed from the same mineralizing fluids which evolved from within the granitoid body and reacted with the host rock, resulting in pyrite and gold precipitation. Bralia *et al.* (1979), and Walsh and Solomon (1981), noted that remobilized pyrites are accompanied by a *decrease* in the Co content while the Ni content remains constant, which characterises the pyritic schists. The slight decrease in Ni content in the schists is attributed to the fact that the Ni was concentrated into the accompanying pyrrhotite phase which was present during later shearing and fluid movement.

The gold content of the pyrites and the element correlations suggests that a portion of the gold occurs either in solution or as sub-microscopic inclusions within the lattice. This indicates simultaneous precipitation of pyrite and gold, or the precipitation of gold from solution onto the pre-existing pyrite lattice.

The extensive cubic pyrites which occur within the mafic and ultra-mafic schists at GEM and other areas in the Murchison, have trace element characteristics which are unrelated to the hydrothermally precipitated pyrites associated with Au-Sb and beryl mineralization. Their high Co and Ni contents confirm that they are likely to be diagenetic or metamorphic in origin.

CHAPTER 5
Stable Isotope Geochemistry

When used in combination with geological and petrographic data, stable isotope measurements can provide useful information about mineral deposits and their environment of formation, including the temperature of formation and the probable source of the fluids. The interpretation of stable isotope data is based on the assumption that equilibrium isotopic fractionation occurred between the mineralizing fluids and the precipitating minerals. The isotopic compositions of sulphur, carbon and oxygen from albitized and mineralized intrusions have been analysed in order to characterise the 'geochemical signature of the fluids involved in the alteration of the intrusions and to test the hypothesis that the fluids involved in the alteration are of a magmatic origin.

Standard notation is used to express the data, where the δ value is the difference in isotopic ratio between the sample and a standard, expressed in parts per thousand, or per mil ($^0/_{00}$).

5.1. Sulphur Isotopes

The isotopic ratios (S^{34}/S^{32}) of sulphur in sulphide minerals have commonly been used to interpret the origin of ore deposits (Ohmoto, 1972). Sulphides of magmatic-hydrothermal origin are assumed to have sulphur isotopic compositions similar to those of sulphides in meteorites ($\pm$ O $^0/_{00}$). Ore deposits which show a wide variation in isotopic composition and which deviate from zero have generally been interpreted as being of biogenic or sedimentary derivation (Jenson 1967). However caution must be excised since, Ohmoto and Rye (1979) have demonstrated that sulphides which precipitate, from magmatic sulphur, for example, can exhibit a wide range of $\delta^{34}S$ values while sulphides precipitated from non-magmatic sources such as sea water, can have a limited range of $\delta^{34}S$ values near 0 $^0/_{00}$ (e.g., the Kuroko deposit).

The sulphur isotopic fractionation between various sulphide minerals and aqueous sulphide species may be used for the determination of physiochemical conditions (Sakai, 1968). However, isotopic equilibrium may continue during sub-solidus cooling and

resulting temperature determinations may represent a chemical event rather than mineralogical one. The sulphide isotope compositions of sulphide minerals may also be used to provide a means of evaluating possible sources of sulphur and may reveal clues about the deposition mechanism. This is possible because of the sensitivity of sulphur isotopic fractionation to changes in the redox conditions, temperature and sulphur concentrations in the fluid (Sakai, 1968).

Although no direct experimental data on isotopic fractionation among sulphide species at magmatic temperatures is available, extrapolation of low temperature data suggests that isotopic fractionation factors among all sulphide species are similar to within 0.5 $^0/_{00}$ (Ohmoto and Rye, 1979). Therefore, magmas formed by partial melting of the mantle, rocks formed from such melts and magmatic gases which escape from such magma, should have $\delta^{34}S$ values similar to those of the parental material. If the mantle has sulphur isotopic composition as homogeneous as that of meteorites, igneous rocks formed by partial melting of the mantle, including the earliest crustal rocks, should also exhibit $\delta^{34}S$ values of $0 \pm 1\ ^0/_{00}$. However, many igneous rocks have $\delta^{34}S$ values outside this range. The non-zero $\delta^{34}S$ values are either due to mantle heterogeneity or to assimilation of crustal sulphur during emplacement of magmatic intrusions. The variation in the S isotopic composition of crustal rocks is largely caused by biological activity and is particularly evident in crustal rocks younger than 2.5 billion years (Ohmoto 1972).

The following points are relevant to the interpretation of $\delta^{34}S$ data:

1. Magmatic sulphur (mantle derived) is generally characterised by $\delta^{34}S$ values concentrated in the narrow range of -3 to $+3\ ^0/_{00}$.
2. Reduced, sulphur-poor, solutions, dissolving magmatically-derived sulphides, should have $\delta^{34}S$ values indistinguishable from magmatic sulphides, but may have a $\delta^{34}S$ value higher than that of the leached pre-existing mineral (up to $+5\ ^0/_{00}$) (Grinenko and Grinenko, 1976) depending on the degree of dissolution.
3. In partially oxidized hydrothermal systems, ^{34}S is strongly enriched in $(SO_4)^{2-}$, which results in negative $\delta^{34}S$ values for the sulphide minerals precipitating by amounts which increase with the proportion of sulphate, down to a theoretical minimum value of -25 $^0/_{00}$ (Ohmoto and Rye, 1979). Fluids having variable SO_2/H_2S ratios would precipitate sulphides having variable $\delta^{34}S$ values.
4. Sulphide minerals precipitated from a fluid dominated by reduced species, without any significant oxidation at the site of deposition, would result in $\delta^{34}S$ values slightly more

positive than that of the fluid and would show small isotopic variations.

5. The isotopic composition of sulphur in hydrothermal minerals is strongly controlled by the fO_2 and the pH values of the hydrothermal fluid, as well as by the temperature and the isotopic composition of sulphur in the fluids. Large variations in the isotopic ratios may be caused by slight variations in the fO_2 and pH of the ore-forming fluid during deposition.

It is, however, difficult to characterize the sulphur isotopic values for all potential sulphur reservoirs unambiguously, because small changes in the temperature, pH and fO_2 can induce large changes in the sulphur isotopic values of the indigenous or derived sulphur-bearing species. Thus, two factors are considered significant in interpreting sulphur isotope data, viz: the average for the deposit as a whole and the variation of $\delta^{34}S$ that occurs *within* the deposit (Ohmoto and Rye 1979).

5.1.1. Archaean Sulphur Isotopes.

Sulphur isotopic data from Archaean gold deposits in Canada have been reported by Wanless *et al.* (1960), Lavigne (1983), Spooner *et al.* (1985), Colvine *et al.* (1988) and Cameron and Hattori (1987). Two broad groupings of $\delta^{34}S$ values have been identified, namely deposits with $\delta^{34}S$ values between 0 and $+10\,^{0}/_{00}$ and those with values less than zero. This division appears to be more transitional than abrupt, and the $0\,^{0}/_{00}$ cut off is a convenient, albeit arbitrary, boundary value (Colvine *et al.*, 1988). The light sulphur values ($<0\,^{0}/_{00}$) may reflect relatively oxidizing hydrothermal fluids, as demonstrated by the presence of sulphate minerals and haematite within the auriferous system (Cameron and Hattori, 1987). This association is not always definitive, however, since for example the McIntyre ore-body, is characterised by the presence of sulphate minerals, but does not have pyrites with distinctly negative $\delta^{34}S$ values. Many deposits display intra-deposit isotopic variation, suggestive of either mixing of more than one fluid source, or major isotopic fractionation. Schwariz and Rees (1985) and Cameron and Hattori (1987) suggest that redox changes within and between deposits, with attendant isotopic fractionation, is the dominant factor contributing to sulphur isotopic variations.

Lambert *et al.* (1984), Golding and Wilson (1983) and Cameron and Hattori (1987) have presented sulphur isotope data for Western Australia. These data show a range from $+0.7$ to $+8.0\,^{0}/_{00}$, which compares favourably with the data for the Canadian deposits which have positive values (Colvine *et al.*, 1988). The $\delta^{34}S$ values for the Golden Mile lodes are, however, notably lower, ranging from -9.0 to $0\,^{0}/_{00}$ (Lambert *et al.*, 1984). This

population is similar to the Canadian deposits which sulphur isotope values less than 0 $^0/_{00}$. Taking into account the specific environments of Archaean gold deposits, the most likely sources of sulphur, in terms of size and availability of reservoir, include direct derivation from magmatic fluids and leaching of primary and secondary sulphide minerals from igneous rock. Unequivocal Archaean marine sulphate deposits with the necessary size to provide the required quantity of sulphur (SO_2^{-2}) are rare. Furthermore,there is seldom a spatial correlation between evaporitic sequences and gold deposits. The $\delta^{34}S$ value for Archaean sulphate deposits is nevertheless near to that of 0 $^0/_{00}$ and indistinguishable from that of magmatic sulphur (Lambert *et al.*, 1978). This leads to the inference that derivation of sulphur in Archaean gold systems involved participation of either magmatic fluids, and/or metamorphic dehydration, or degassing of the underlying rock column.

The general similarity between sulphur isotope distributions in various Archaean greenstones emphasizes the probability of a uniform sulphur source. The range of $\delta^{34}S$ data within the pyrites may be accounted for by the partitioning between oxidized and reduced sulphur species in the hydrothermal fluid (Schwarcz and Rees, 1985). Given these constraints, the relatively confined grouping of the bulk of Archaean sulphur isotopic data to within +1 to +6 $^0/_{00}$, may be interpreted as an involvement of fluids dominated by reduced sulphur species (magmatic or metamorphic), with only limited oxidation accompanying precipitation (Lambert *et al.*, 1984). The negative values which are found in some Archaean gold deposits (eg. Golden Mile) can be attributed to the physiochemical conditions of the hydrothermal system in particular the fO_2 (Cameron and Hattori, 1987). A $\delta^{34}S$ of about 0 $^0/_{00}$ for the total dissolved sulphur in auriferous fluids is consistent with, and capable of yielding, the observed $\delta^{34}S$ values in Archaean gold deposits, given appropriate reducing or oxidizing conditions at the site of deposition. This isotopic composition may be interpreted as suggesting that the parental fluid contained magmatic sulphur. However, this magmatic sulphur may have entered the fluid phase either by dissolution of juvenile sulphide minerals by metamorphic fluids, or by direct contribution from magmatic sources. Neither process is discriminated unequivocally by the sulphur isotopic data. It should be noted, however, that sulphides with $\delta^{34}S = \pm 0\,^0/_{00}$ need not have precipitated from solutions in which the isotopic ratio of the total sulphur is also $\pm 0\,^0/_{00}$ due to fractionation (Ohmoto, 1972).

5.1.2. Sulphur Isotope Preparation.

All sulphur isotope analyses were undertaken by the author at the University of the Witwatersrand, using conventional SO_2 extraction facilities in the Department of Geology and the mass spectrometer at the Schonland Research Centre for Nuclear Sciences. The sulphur isotope line utilizes the Cu_2O-oxidation method of Fritz *et al.* (1974), Robinson and Kusakabe (1975) and Coleman and Moore (1978). This technique is designed to minimize elemental sulphur and SO_3 production and also to limit any equilibrium fractionation between Cu_2O and SO_2. The function of the line is to convert sulphide to pure sulphur dioxide. The sulphide samples can be run directly, with no sample preparation required, which reduces the chance of fractionation effects during sample preparation. The sulphur line produces sulphur dioxide gas, free of air, SO_3, H_2O and CO_2. The presence of any of these gases will result in a considerable error in the ratio measurement in the dual inlet mass spectrometer. The minimum quantity of sulphur required for precision work is 5 mg, which equates to approximately 9-10 mg of pyrite. Pyrites were obtained by the dissolution of the silicate matrix with hydrofluoric acid, and these were subsequently examined under a binocular microscope to minimize the inclusion of other phases of sulphide minerals in the analysis. The reproducibility of the extraction facility and mass spectrometer has been found to be within 0.2 $^0/_{00}$ about the mean. All results are expressed relative to the S^{34}/S^{32} ratio of the Canyon Diablo troilite (CD), in which the S^{34}/S^{32} ratio is defined as 0.0450045 (Jenson and Nakai, 1963) and:

$$\delta^{34}S\ ^0/_{00} = \frac{(^{34}S/^{32}S)i - (^{34}S/^{32}S)std \times 1000}{(^{34}S/^{32}S)std}$$

where i = the ratio of the sample.

The reference gas used with the mass spectrometer is calibrated and checked against reference gases prepared by oxidizing a laboratory standard in the same way as the samples, so as to reduce oxygen isotopic differences to a minimum. Reference samples are run through the line after every five samples to monitor for variations in the extraction method and for problems with the mass spectrometer. The necessary corrections and conversions of the mass spectrometer readings, to produce $\delta^{34}S$ values relative to Canyon Diablo are carried out by a computer programme attached to the mass spectrometer. The most important part of the extraction of SO_2 gas is monitoring the yield of SO_2 gas and to ensure a complete yield, so as to avoid kinetic fractionation. All samples were run in duplicate to check for fractionation effects.

5.1.3. Previous Isotope Studies in the Murchison Schist Belt.

As the major mineralization in the Murchison schist belt is associated with the Antimony Line, previous stable isotopic studies have concentrated on this region. Sulphur isotope work on the ores of the Monarch mine was undertaken by Pearton and Viljoen (1986), in an attempt to define the nature and origin of the mineralizing fluid. Their results were not diagnostic and did not indicate a definitive source for the fluids responsible for mineralization. The $\delta^{34}S$ values for stibnite from the Monarch mine, lie in the range 1.4 to 3.7 $^{0}/_{00}$ with an average of 2.6 $^{0}/_{00}$. They did not observe any isotopic fractionation between the primary and remobilized phase of stibnite mineralization, nor did they detect any isotopic variation across the mineralized lode. They proposed that the values obtained are consistent with both a magmatic exhalative, or a magmatic hydrothermal (including remobilized magmatic) source. The narrow range of the values favours an epigenetic emplacement of sulphur.

Pearton and Viljoen (1986) also obtained data from four berthierite and three pyrite samples from the Antimony Line. The $\delta^{34}S$ results were lower than from the stibnite. They proposed that since the pyrite and berthierite values are at the outer range of the stibnite values, it is likely that the antimony ore fluids reacted with pre-existing pyrite in the host rocks, resulting in berthierite with an intermediate composition. What the authors have not considered are the effects of isotopic fractionation between the various mineral phases and dissolved sulphur phases. The exact $\delta^{34}S$ fractionation factors for sulphur species dissolved into the stibnite phase is not known, but is likely to be greater than that of pyrite. It is thus possible that under specific physiochemical conditions, a single sulphur bearing fluid may be responsible for the mineralization of pyrite, berthierite and stibnite, with $\delta^{34}S$ variations between the minerals being due to standard isotopic fractionation effects (Ohmoto and Rye, 1979) and not different stages of sulphur input as proposed by Pearton and Viljoen (1986).

5.1.4. Sulphur Isotope Determinations in the Present Study.

Samples of pyrite from the albitized intrusions at Discovery Shaft, Malati Store and Minerva mine, as well as the spatially related auriferous pyritic schists at Discovery Shaft and Minerva mine were analysed. Three samples of pyrite from the Antimony Line were also analysed to compare with Pearton and Viljoen's (1986) data. Pyrites from the albite pegmatites in the Cobra and Discovery pit at GEM were also extracted and analysed. A pyrite-molybdenum intergrowth from the Discovery Shaft intrusion was separated and analysed to determine whether the isotopic ratios reflect a condition of equilibrium

fractionation.

5.1.5. Results.

The $\delta^{34}S$ results of this study are presented in Table 5.1.1 and a statistical treatment of the data is presented in Table 5.1.2. The results given are the average of duplicate samples. The entire $\delta^{34}S$ values ranges between +3.95 and -1.60 $^0/_{00}$. Pyrites from the albitized intrusions have similar $\delta^{34}S$ values and fall within a narrow range (± 2.5 $^0/_{00}$). The Discovery Shaft intrusion has an average $\delta^{34}S$ of 1.48 ± 0.66 $^0/_{00}$ (n = 16, mode = 1.50). Two values were excluded from the average at a 99% confidence limit. The Malati Store intrusion has an average $\delta^{34}S$ of 1.28 ± 0.66 $^0/_{00}$ (n = 19, mode = 2.1). One sample was excluded from the average at a 99% confidence limit. Using the students "t" test, the $\delta^{34}S$ values from the two intrusions are statistically similar at a 95% confidence limit. The limited samples from the Minerva Mine intrusion and the albite pegmatites from GEM indicate that the samples are statistically similar to the Malati Store and Discovery Shaft intrusions at a 95% confidence limit.

The isotopic ratio of the sulphur from the intrusions occurs within the range considered to represent that of magmatic sulphur. The distinct similarity between the $\delta^{34}S$ values for the different intrusions, suggest that a common fluid was responsible for the precipitation of pyrite and that similar physiochemical conditions prevailed during the alteration and precipitation of the pyrite within the intrusions. The slightly positive values and the narrow range of these values suggest that the fluids responsible were dominated by reduced sulphur species and only minor oxidation occurred at the site of pyrite deposition, suggesting fairly constant fO_2 conditions. The similarity between the $\delta^{34}S$ values of the albite pegmatites and the altered intrusions confirms suggestions that the fluids are genetically related.

The pyrite from the auriferous pyritic schist at Discovery Shaft has a lower average $\delta^{34}S$ value and a wider range of $\delta^{34}S$ values, than the intrusions. The pyritic schists average $\delta^{34}S$ is -0.43 ± 1.32 $^0/_{00}$ (n = 16, mode = -0.95 $^0/_{00}$). The limited samples from the Minerva mine pyritic schist also indicate a spread of values, and include negative values. The $\delta^{34}S$ average is near 0 $^0/_{00}$, which indicates that similar sulphur bearing fluids to those responsible for mineralization within the intrusion were involved in the precipitation of the pyrite within this ore zone.

Malati Stock Intrusion (MSI)	
Sample	$\delta^{34}S$
DIS.1	4.23*
DIS.2	0.65
DIS.3	1.36
DIS.5	1.86
KE.21	1.25
KE.81.1	0.09
KE.81.2	0.99
KE.180	0.63
KE.180.2	1.15
KE.180.3	1.55
KE.81.3	2.10
DIS.8	1.10
DIS.8.2	0.01
DIS.8.3	2.10
DIS.8.4	0.84
DIS.3.4	1.56
DIS.3.5	1.54
DIS.12.1	1.20
DIS.12.2	1.90
DIS.12.3	2.50
Average	1.28

Discovery Shaft Intrusion (DSI)	
Sample	$\delta^{34}S$
MM2.13	-3.54*
MM2.161	4.70*
MM3.185	1.56
MUL.1	1.25
MUL.2	1.30
MUL.3	2.50
MUL.4	0.45
MUL.5	1.90
MUL.6	1.11
MM2.165	0.59
MM2.156	0.23
MM4.143	1.89
MM4.145	1.42
MMD.1	1.69
MMD.2	1.84
MM1.45	2.20
MM1.150	2.40
MM1.189	1.50
Average	1.48

Discovery Pyritic Schist (DPS)	
Sample	$\delta^{34}S$
3.3	-4.65*
7.2	0.05
7.3	0.25
7.4	0.36
7.5	1.98
7.6	1.50
10.1	-0.60
10.2	-0.86
10.3	-1.30
3.1	-0.34
3.2	-2.70
3.3	-2.1
6.5	-1.60
6.6	0.95
6.7	-0.95
4.4	-1.23
4.4	1.60
Average	-0.43

* - Samples rejected at a 99% confidence limit

Minerva Mine Intrusion (MMI)	
Sample	$\delta^{34}S$
MIN.2	2.20
MIN.4	1.67
MIN.4A	2.34

Minerva Pyritic Schist (MPS)	
Sample	$\delta^{34}S$
MDM.3	-0.05
MDM.2	-1.20
MDM.12	-1.31

Albite Pegmatites (ABP)	
Sample	$\delta^{34}S$
CBR.1	1.15
CBR.2	0.25
DIP.2	1.59

Antimony Line Pyrite (ALP)	
Sample	$\delta^{34}S$
ANT.4	-1.25
MON.1	1.45
MON.2	1.39

Table 5.1.1. RESULTS OF $\delta^{34}S$ ISOTOPIC STUDY FOR PYRITES RELATIVE TO CANYON DIABLO

Statistics	MSI	DSI	DPS
Sample Size	19	16	16
Average	1.28	1.48	-0.43
Median	1.25	1.53	-0.73
Mode	2.1	1.50	-0.95
Geometric Mean	0.89	1.28	-
Std. Deviation	0.66	0.66	1.32
Minimum	0.01	0.23	-2.70
Maximum	2.5	2.50	+1.98
Range	2.49	2.27	4.68

MSI = Malati Store intrusion
DSI = Discovery Shaft intrusion
DPS = Discovery Shaft pyritic schist

Table 5.1.2. STATISTICS OF SULPHUR ISOTOPE RESULTS RELATIVE TO CANON DIABLO ($\delta^{34}S$ PER MIL)

The larger range in values, apparently to lower $\delta^{34}S$ values, suggest that changing physiochemical conditions occurred within the zone of precipitation. This is most likely due to changes in the fO_2, caused by redox reactions occurring at the site of pyrite deposition. The pyrite samples from this study of the Antimony Line have an average $\delta^{34}S$ value of 0.53 $^0/_{00}$ (n= 3) and a range of -1.25 to 1.39 $^0/_{00}$. The limited data, along with the data of Pearton and Viljoen (1986) indicate that the pyrites have a large range of values possibly to more negative values. This value is similar to the average values from the Discovery Shaft schist suggesting that variations in the fO_2 also occurred during sulphide precipitation within the Antimony Line.

The sulphur isotopes of the pyrites from the albite pegmatites at GEM associated with emerald mineralization are statistically similar to the pyrites from the albitized intrusions indicating a genetic relationship.

5.1.6. Sulphide Precipitation Temperature

The pyrite - molybdenite intergrowth from the Discovery Shaft intrusion have average $\delta^{34}S$ values of 1.54 $^{0}/_{00}$ (n=2) and 2.13 $^{0}/_{00}$ (n=2) respectively.

The experimental $\delta^{34}S$ fractionation data of Survorova (1974) for the molybdenite - pyrite system, indicate that at temperatures below 520°C,

$$\delta^{34}S_{molybdenite} > \delta^{34}S_{pyrite}.$$

ie.$^{*}\delta^{34}S$ is positive

The $\delta^{34}S$ - temperature relationship for the molybdenite-pyrite fractionation is negatively sloped so that at low temperatures $\delta^{34}S_{molybdenite} >> \delta^{34}S_{pyrite}$. The $\delta^{34}S$ values for molybdenite and pyrite from the Discovery Shaft indicate possible equilibrium fractionation ($^{*}\delta^{34}S$ = +0.59). Use is made of the equilibrium fractionation relationship from Survorova (1974) to calculate the equilibrium precipitation temperature.

$$10^{3} \ln\alpha = 0.48(10^{6}\ T^{-2}) - 0.75$$

Molybdenite $\delta^{34}S$ = +2.09 $^{0}/_{00}$
Pyrite $\delta^{34}S$ = +1.54 $^{0}/_{00}$
$^{*}\delta^{34}S$ = +0.55 $^{0}/_{00}$

Where $10^{3} \ln\alpha \approx {}^{*}\delta^{34}S \approx \delta^{34}S_{moly} - \delta^{34}S_{pyrite}$

Temperature = 335°C

No third sulphide phase was available to confirm the apparent equilibrium temperature of 335°C

5.1.7. $\delta^{34}S$ Comparison With Other Archaean Gold Deposits

Figure 5.1.1 is a compilation of available $\delta^{34}S$ data from pyrites directly associated with gold mineralization from a variety of Archaean deposits compared to the $\delta^{34}S$ values from this study. The results of this study compare favourably with data from other Archaean mesothermal gold deposits.

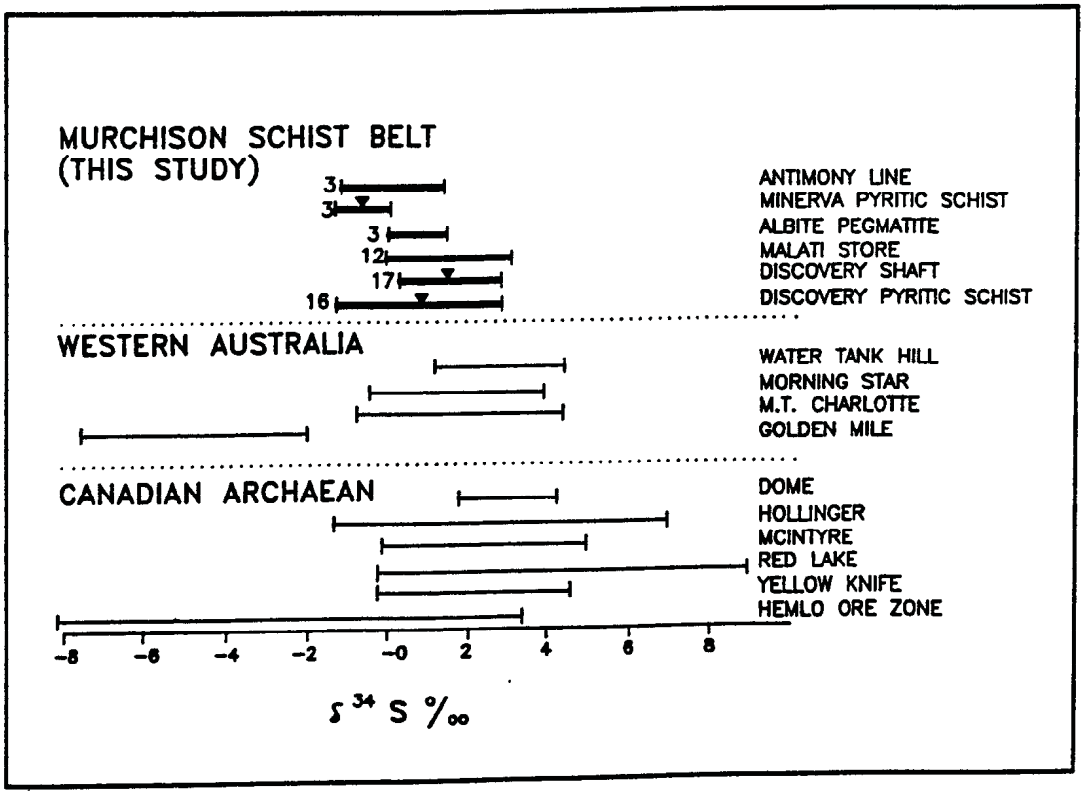

Figure 5.1.1. Sulphur isotope values from pyrite from this study compared to $\delta^{34}S$ values of pyrite from other Archaean gold deposits. (Adapted from Colvine *et al.*, 1988)

5.1.8. Conclusions

The sulphur isotope data indicate that the fluids responsible for alteration and pyrite mineralization contained reduced sulphur complexes at temperatures of approximately 335°C. The $\delta^{34}S$ values are consistent with a magmatic origin of the sulphur under moderately reduced conditions, although leaching of pre-existing magmatic sulphides cannot be discounted. Similar $\delta^{34}S$ values for the albite pegmatites infer a genetic relationship between the fluids responsible for mineralization within the intrusions and those involved in the development of the pegmatites. The greater spread of values, including progression to negative $\delta^{34}S$ values for the auriferous pyritic schists and Antimony Line is probably due to oxidation reactions occurring during fluid interaction with the country rocks at the site of deposition. The range in $\delta^{34}S$ values for the pyrites from the Antimony Line studied by Pearton and Viljoen (1986) and in this study indicate that changes in fO_2 may also have occurred during the precipitation of sulphides along the Antimony Line. This change in fO_2 during wall rock alteration and pyrite precipitation is further described in Section 5.4.

Since the various intrusions occur in different geological settings and with some distance separating them, mineralizing fluids with similar $\delta^{34}S$ isotopic compositions must have acted over large areas of the schist belt under similar physiochemical conditions. This suggests that a large, isotopically homogeneous source, was responsible for the derivation of the sulphur.

The similarity between the $\delta^{34}S$ compositions of the pyrites from the Antimony Line and those within the granitoids suggests that similar fluids were responsible for the mineralization along this major structural feature.